Case Studies in Thermal Engineering 34 (2022) 101915

Contents lists available at ScienceDirect

Case Studies in Thermal Engineering

journal homepage: www.elsevier.com/locate/csite

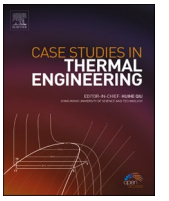

On the influence of environmental boundary conditions on surface thermal resistance of walls: Experimental evaluation through a Guarded Hot Box

Tullio de Rubeis [a,*], Luca Evangelisti [b], Claudia Guattari [c], Pierluigi De Berardinis [d], Francesco Asdrubali [b], Dario Ambrosini [a]

[a] University of L'Aquila, Department of Industrial and Information Engineering and Economics (DIIIE), Piazzale Pontieri 1, Monteluco di Roio, I 67100, L'Aquila, Italy
[b] Roma TRE University, Department of Industrial, Electronic and Mechanical Engineering, Via Vito Volterra 62, 00146, Rome, Italy
[c] Rome TRE University, Department of Engineering, Via Vito Volterra 62, 00146, Rome, Italy
[d] University of L'Aquila, Department of Civil, Construction-Architectural and Environmental Engineering (DICEAA), Piazzale Pontieri 1, Monteluco di Roio, I 67100, L'Aquila, Italy

HIGHLIGHTS

- Influence of environmental boundary conditions on walls surface thermal resistance.
- Assessment of the convective heat transfer in function of the air speed through GHB.
- Comparison between experimental data and conventional values provided by ISO6946.

ARTICLE INFO

Keywords:
Internal surface thermal resistance
Convective and radiative heat transfer
Guarded hot box

ABSTRACT

In this work, a Guarded Hot Box (GHB) was employed to evaluate the effects of environmental boundary conditions on the internal surface thermal resistance of a wall. For this purpose, the study was carried out through an experimental setup to measure temperature - surface and ambient - in the two chambers of the GHB and air velocity near the specimen wall in the hot chamber. The experimental analysis together with the analysis of the dimensionless parameters allowed to determine the internal convective coefficient for different air speeds. To evaluate the results obtained with the proposed methodology, some existing correlations for the determination of the convective coefficient were used. Moreover, the measurement of the emissivity of sample surface and baffle, and the determination of the mean radiant absolute temperature allowed to calculate the radiative coefficient. Therefore, the internal surface thermal resistance with different air velocities, given by the combination of convective and radiative heat transfer, was determined, and compared with the value offered by the standard ISO 6946.

1. Introduction

One of the largest energy consumers is the building sector [1]. In Europe buildings are responsible for 40% of energy consumption and 36% of greenhouse gas emissions [2,3]. Improving buildings energy efficiency is therefore essential to achieve the ambitious goal

* Corresponding author.
E-mail address: tullio.derubeis@univaq.it (T. de Rubeis).

https://doi.org/10.1016/j.csite.2022.101915
Received 30 September 2021; Received in revised form 21 February 2022; Accepted 2 March 2022
Available online 14 April 2022

of carbon neutrality, as defined in the European Green Deal [4]. Nevertheless, energy retrofit is strictly related to the assessment of the actual performance of buildings [5]. This concept passes through the comprehension of the thermal behavior of building components [6]. The thermal characterization of structures allows to understand the impact of energy saving measures [7,8]. In existing buildings, this is essentially related to experimental investigations able to provide information related to walls thermal resistance (R-value) or thermal transmittance (U-value) [9]. Several experimental approaches can be applied to obtain the R-value or U-value of walls [10]. The heat-flow meter method is the widely used, but other quite new methods could be applied [10]. Among them, the thermometric method [11] requires the heat flux calculation by means of an indirect approach, based on the environment-wall total heat transfer coefficient. As an immediate approach, for horizontal heat flux, the total heat transfer coefficient suggested by the ISO 6946, equal to 7.69 W/m^{2}K, could be used. This is a constant value, characterized by a convective component equal to 2.5 W/m^{2}K and a radiative part equal to 5.19 W/m^{2}K. However, the question is whether these coefficients can be considered representative for any environmental condition.

The heat flux between a fluid and a solid is a function of the surface thermal resistance, whose estimation needs the knowledge of several parameters. Finding the proper value is demanding, requiring a suitable experimental apparatus [12]. The selection of suitable convective heat transfer coefficient affects the assessment of buildings thermal comfort and energy consumption. Nowadays, several established analytical and experimental correlations can be found in literature, accounting different flow types and ventilation modes, both for internal [13] and external surfaces [14].

In 2015, Obyn et al. [15] investigated the influence of different convective heat transfer coefficient correlations on heating and cooling loads of a building modelled via TRNSYS software. A classification of the existing expressions was done, concluding that the impact of specific expressions on HVAC design is quite limited for light walls but is greater for heavy masonries. Otherwise, the use of constant values seems to be acceptable, although in some cases there are deviations in the heating demand up to about 9%. Moreover, the author observed that large differences occur in the average value of the annual coefficient, as already noted by Khalifa in 2001 [16]. The convective coefficient has a real effect on the assessment of the energy performance of a building, as already observed by Mirsadeghi et al. [17]. From an experimental point of view, in 2016, Evangelisti et al. [18] investigated the convective heat flux obtained from five different existing correlations, as well as its influence on the thermal transmittance. They observed that the similarity-based correlations allow to compute convective coefficients values significantly different from the constant one suggested by the ISO 6946.

Later, in 2019, Bienvenido-Huertas et al. [19] applied 45 correlations of internal convective heat transfer coefficients for the quantitative internal infrared thermography method, concluding that the use of convective coefficients depending on dimensionless numbers is the most efficient approach.

Recently, in 2021, Camci et al. [20] provided a comparative review related to the progress of convective heat transfer at indoor applications. They assessed mostly experimental correlation studies, highlighting that mixed convection has not been widely investigated from an experimental point of view. In their work, they included all convection types with descriptions, explanations, and comparisons.

In the same year, Piotr Michalak [21] carried out an experimental and theoretical study on the internal convective and radiative heat transfer coefficients in a residential building. He observed that experimental investigations on internal convective and radiative coefficients are rarely carried out in actual conditions.

On the other hand, it is worthy to observe that climatic chambers allow to obtain controlled environmental boundary conditions. For this reason, here a Guarded Hot Box (GHB) was used for assessing the influence of specific environmental boundary conditions on the surface thermal resistance of a wall. For this purpose, several sensors were installed in the GHB. The experimental approach, together with the dimensionless parameters' theory, allowed to compute the internal convective coefficient for different air velocity values. Thus, the objective of this work is the internal surface thermal resistance assessment (given by the convective and radiative heat transfer combination) in function of the air speed, also providing a comparison with the widely used value suggested by the standard ISO 6946 [22]. The novelty of this work is applying a methodological approach based on dimensionless parameters for providing new correlations between convective internal heat transfer coefficient and air speed, also under mixed convection conditions. The approach here proposed could also be applied for those quite new experimental techniques, such as the thermometric method, which requires the total air-wall heat transfer coefficient knowledge. The investigated methodology can free users from the arbitrary selection of a specific coefficient value, suggesting a data processing for the calculation of the most suitable total heat transfer coefficients in function of the specific boundary conditions.

2. Materials and methods

2.1. Theoretical approach

Typical thermal tests of multilayer components are performed through a hot box apparatus according to the standards ISO 8990 [23]. The GHB is characterized by two chambers between which the sample wall is positioned. Hot chamber and cold chamber are brought to very different temperatures. The hot chamber is in turn characterized by a metering box enclosed in a guard box. In the metering box, a baffle is installed in front of the sample wall for providing a radiating surface of uniform temperature. From a theoretical point of view, it is well-known that for multilayer walls, the total thermal resistance (R) is given by the sum of the conductive resistances of each layer (R_i) and the internal (R_{si}) and external (R_{se}) surface resistances [24], as shown by Eq. (1):

$$R = R_{si} + \sum_i R_i + R_{se} \tag{1}$$

According to the standard ISO 8990, the surface resistances, characterized by the combination of convective and radiative heat transfer, can be computed by applying Eq. (2):

$$R_s = \frac{1}{h_c + E \cdot h_r} = \frac{1}{h_{tot}} \tag{2}$$

where h_c is the convective heat transfer coefficient, h_r is the radiative heat transfer coefficient, E is the emissivity factor, and h_{tot} is the total heat transfer coefficient. In particular, h_r can be computed applying the following formula:

$$h_{ro} = 4 \cdot \sigma \cdot T_m^3 \tag{3}$$

where σ is the Stefan-Boltzmann's constant ($5.67 \cdot 10^{-8}\ W/m^2K^4$) and T_m is the mean radiant absolute temperature, given by Eq. (4).

$$T_m^3 = \frac{\left(T_r'^{\,2} + T_s^2\right) \cdot \left(T_r' + T_s\right)}{4} \tag{4}$$

where T_r' is the mean radiant temperature seen by the specimen (i.e., the mean baffle temperature) and T_s is the surface temperature of specimen wall.

If a baffle is installed close and parallel to the sample wall, the emissivity factor (E) can be determined by Eq. (5).

$$E = \frac{1}{\frac{1}{\varepsilon_1} + \frac{1}{\varepsilon_2} - 1} \tag{5}$$

where ε_1 and ε_2 are the emissivity of the sample and baffle, respectively.

Considering the convective heat transfer between walls and air, the Newton's law of cooling [24] can be applied for quantifying the convective heat flux (q_c) transferred between the wall surface and air, according to the following formula:

$$q_c = h_c \cdot (T_s - T_a) \tag{6}$$

where T_s is the wall surface temperature, T_a is the air temperature and h_c is the convective heat transfer coefficient. As known, convective heat transfers are quantified by the convective coefficients. In turn, h_c can be obtained by means of the dimensionless parameter's theory [24], based on the calculation of Grashof (Gr) and Reynolds (Re) numbers for better comprehending if natural or forced convection occur. Therefore, h_c is also a function of the air speed brushing the wall. Given the complexity of thermal and fluid dynamics phenomena, several correlations can be found in literature for the h_c calculation, based on similarity-based and experimental expressions. Most of these correlations have been derived from a flat plate configuration [25,26] or from tests in thermally controlled rooms [27,28].

The type of convection that occurs can be identified by means of the Richardson number, also known in building physics applications as Archimedes (Ar) number [29]:

$$Ar = \frac{Gr}{Re^2} \tag{7}$$

The calculation of Ar is fundamental to understand the correlation to be applied to compute the Nusselt (Nu) number. Generally, when Ar number is much lower than 0.7, the convection is forced. When the Ar value is in the range from 0.7 to 10, the convection is mixed. On the contrary, when Ar is greater than 10, the convection is natural. Nu number can be calculated by applying the different

Table 1
Correlations available based on the Ar number [24].

Convection	Archimedes number range	Nu correlation
Natural	$Ar \gg 10$	$Nu = 0.59 Ra^{\frac{1}{4}}$ *for* $10^4 < Ra < 10^9$
		$Nu = 0.10 Ra^{\frac{1}{3}}$ *for* $10^9 < Ra < 10^{13}$
		$Nu = \left\{ 0.825 + \frac{0.387\, Ra^{\frac{1}{6}}}{\left[1 + \left(\frac{0.492}{Pr}\right)^{\frac{9}{16}}\right]^{\frac{8}{27}}} \right\}^2 \forall Ra$
Mixed	$0.7 < Ar < 10$	$Nu^3 = Nu_{forced}^3 + Nu_{natural}^3$
Forced	$Ar \ll 0.7$	$Nu_{forced}^{LAM} = 0.664 Re^{\frac{1}{2}} \cdot Pr^{\frac{1}{3}}$ *for* $Re < 5 \cdot 10^5$ *and* $Pr > 0.6$
		$Nu_{forced}^{TURB} = 0.037 Re^{0.8} \cdot Pr^{\frac{1}{3}}$ *for* $5 \cdot 10^5 \leq Re \leq 10^7$ *and* $0.6 \leq Pr \leq 60$

h_c can be found through the Nu number, as highlighted by the following formula [24].

correlations listed in Table 1. Under natural convection conditions, *Nu* can be computed in function of the Rayleigh (Ra) number. Under forced convection conditions, *Nu* is a function of both Reynolds and Prandtl (Pr) numbers. Finally, when mixed convection occurs, both natural and forced convection take on significance [24].

$$Nu = \frac{h_c \cdot L_c}{\lambda} \tag{8}$$

where L_c is the characteristic geometrical length and λ is the thermal conductivity of air.

As mentioned before, finding the proper h_c value is demanding, requiring a suitable experimental apparatus. Nowadays, several established correlations can be found in literature, some of which, shown in Table 2, were used in this work for comparison with the results obtained from the proposed methodology.

In the absence of specific information on boundary conditions, ISO 6946 suggests using specific R_s values. Considering horizontal heat flux, the standard ISO 6946 suggests a value of internal surface thermal resistance (R_{si}) equal to 0.13 m^2K/W, obtained with a total heat transfer coefficient (h_{tot}) of 7.69 W/m^2K. The value provided by the standard, determined considering a hemispherical emissivity of the surface (ε) equal to 0.9 and a convective coefficient (h_c) equal to 2.5 m^2K/W, does not supply any additional detail regarding the influence of environmental boundary conditions.

2.2. Methodology

Once stationary thermal conditions were reached inside the GHB, the following methodology was applied. As mentioned before, the ISO 6946 suggests a specific value for the convective coefficient (2.5 W/m^2K), not providing information on the boundary conditions that make the use of this value valid. Consequently, researchers and technicians could apply this value in any environment, characterized by radiators, fan coils or air conditioning systems [18]. For this reason, here the h_c coefficients were computed forcing the setup with different air velocity values inside the hot chamber. This was allowed by means of fans able to progressively modify the air flows. Therefore, a hot wire anemometer was used for measuring air speed in proximity of the wall surface. Air and surface temperature probes were also used to measure both air temperatures and wall and baffle surface temperatures in the hot chamber. All data was used for calculating the *Ar* number, thus comprehending the type of convection, and applying the suitable correlation for the *Nu* calculation. Moreover, the existing correlations shown in Table 2 were used to compare the results obtained from the proposed methodology for determining the convective heat transfer coefficient. Each test was conducted for 24 h, thus logging experimental data under stationary boundary conditions, with a data acquisition time equal to 10 min. The emissivity of wall and baffle were measured using infrared thermography and a black tape as reference (characterized by known emissivity) [30], and the mean radiant absolute temperature allowed to obtain h_{ro} by applying Eq. (3). Convective and radiative coefficients were then used to calculate R_s related to the hot surface of the wall. Consequently, the effects of different environmental boundary conditions on the surface thermal resistance were identified, finding a correlation between surface thermal resistance and air velocity. Fig. 1 shows the flow-chart of the methodological approach.

2.3. Experimental setup

The experimental analysis has been carried out using the GHB of the University of L'Aquila [31,32]. The GHB consists of two chambers between which the sample wall is stressed by known and controlled temperature difference, obtained through electrical resistances (hot chamber) and refrigerant unit (cold chamber). The hot chamber is in turn characterized by a metering box enclosed in a guard box. A simplified view of the GHB is shown in Fig. 2a.

As shown inFig. 2b, the GHB and sample wall were equipped with air and surface temperature probes (T_{air} and T_s, respectively) and a hot wire anemometer (*AN*). The technical specifications of the measuring instruments are listed in Table 3. The sample wall, frequently used in the building sector, is made of X-lam panel with double insulation – internal and external – realized with mineral wool and expanded polystyrene (EPS) with graphite, respectively. The complete stratigraphy of the wall is shown in Fig. 3.

2.4. Uncertainty analysis

The uncertainty evaluation was performed following the Holman's method [33] for complicated data reduction. The estimation of the uncertainty can be done based on the uncertainties in the primary measurements. Considering the result *R* of the independent

Table 2
Correlations employed to determine the convective heat transfer coefficient [20].

Reference	Correlation	Remark
ASHRAE	$h = 1.33\left(\frac{\Delta T}{H}\right)^{1/4}$	$10^5 < Ra < 10^9$
	$h = 1.26(\Delta T)^{1/3}$	$Ra < 10^9$
Churchill and Chu	$h = \frac{0.0175}{H} + 1.31\left(\frac{\Delta T}{H}\right)^{1/4}$	Vertical plate
	$h = \frac{0.0175}{H} + 0.28\left(\frac{\Delta T}{H}\right)^{1/4}$	
Khalifa and Marshall	$h = 2.30(\Delta T)^{0.24}$	Wall heating
	$h = 2.92(\Delta T)^{0.25}$	Wall heating (opposed wall)

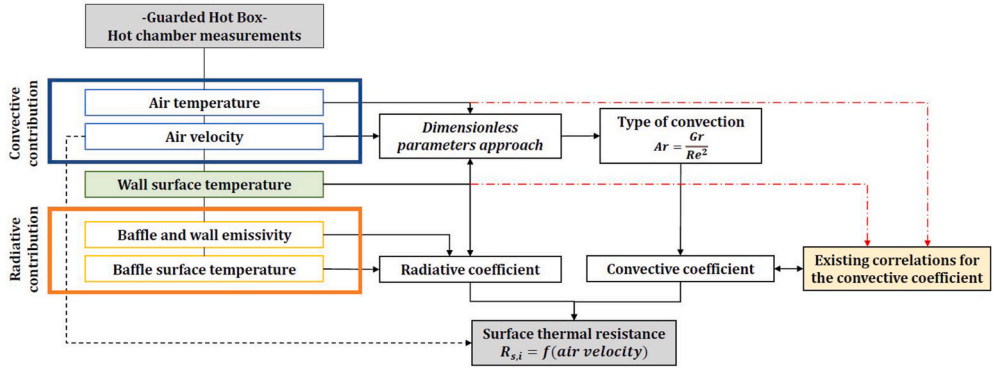

Fig. 1. Flow-chart of the methodological approach.

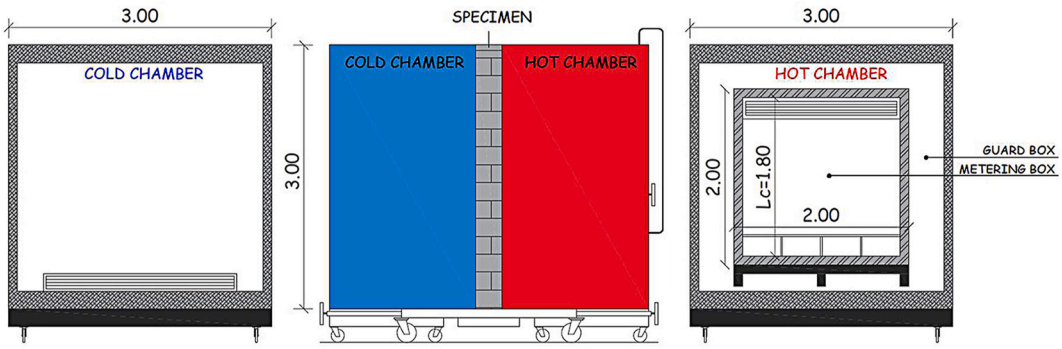

Fig. 2a. The Guarded Hot Box: (a) simplified view (dimensions in meters and L_c is the characteristic geometrical length),

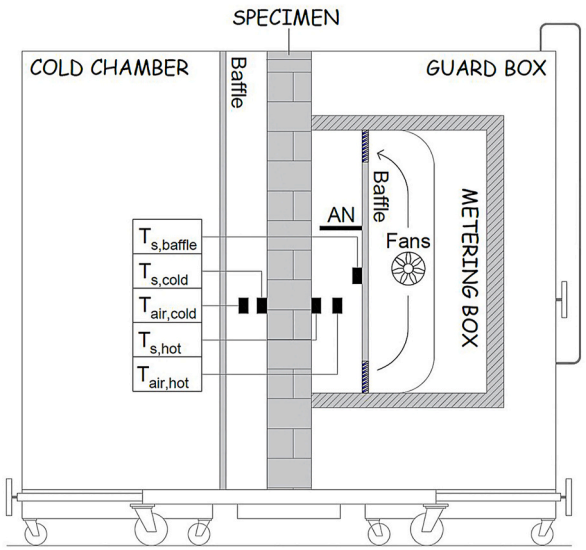

Fig. 2b. (b) experimental setup.

Table 3
Measuring instruments technical data.

Sensor	Manufacturer	Measuring range	Resolution
Surface temperature sensors	LSI Lastem EST124-Pt100	−50 to +70 °C	0.01 °C
Air temperature sensors	Maxim Integrated DS18B20	−55 to +125 °C	0.0625 °C
Hot-wire anemometer	LSI Lastem ESV107	0.01 to 20 m/s	0.01 m/s
Datalogger	LSI Lastem M-Log ELO008	−300 to +1200 mV	40 μV

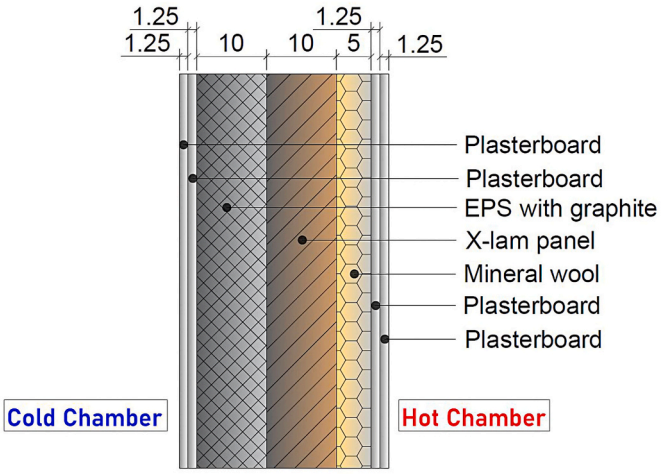

Fig. 3. The sample wall stratigraphy (dimensions in centimeters).

variables $x_1,\ x_2, \ldots, x_n$, it is possible to define R as follows:

$$R = R(x_1,\ x_2, \ldots,\ x_n) \tag{9}$$

Defined w_R the uncertainty in the result and defined $w_1,\ w_2, \ldots,\ w_n$ the uncertainties in the independent variables, if the latter are all given with the same probabilities, then the uncertainty in the result with these probabilities can be computed as:

$$w_R = \sqrt{\left[\left(\frac{\partial R}{\partial x_1}\cdot w_1\right)^2 + \left(\frac{\partial R}{\partial x_2}\cdot w_2\right)^2 + \ldots + \left(\frac{\partial R}{\partial x_{n1}}\cdot w_n\right)^2\right]}\sqrt{a^2+b^2} \tag{10}$$

An adaptation can provide for the direct calculation of uncertainties without resorting to an analytical calculation of the partial derivatives in Eq. (10). Supposing a set of data collected in the variables $x_1,\ x_2, \ldots, x_n$ and a calculated result. One may perturb the variables by $\Delta x_1,\ \Delta x_2$, and so on, thus calculating new results. The following equations can be written:

$$R(x_1) = R(x_1,\ x_2, \ldots,\ x_n) \tag{11}$$

$$R(x_1 + \Delta x_1) = R(x_1 + \Delta x_1,\ x_2, \ldots,\ x_n) \tag{12}$$

$$R(x_2) = R(x_1,\ x_2, \ldots,\ x_n) \tag{13}$$

$$R(x_2 + \Delta x_2) = R(x_1,\ x_2 + \Delta x_2, \ldots,\ x_n) \tag{14}$$

Considering small values of Δx, the partial derivatives can be approximately rewritten as:

Table 4
Operating conditions of experimental campaign.

Test	Average air velocity [m/s]	Average air temperature hot chamber [°C]	Average sample surface temperature (hot side) [°C]	Average baffle surface temperature (hot chamber) [°C]	Average air temperature (cold chamber) [°C]
T1	<0.009*	20.13 ± 0.09	19.04 ± 0.03	20.18 ± 0.07	−0.16 ± 0.21
T2	0.064 ± 0.010	19.97 ± 0.19	18.80 ± 0.01	19.59 ± 0.15	−0.16 ± 0.21
T3	0.089 ± 0.010	20.00 ± 0.31	18.97 ± 0.05	19.90 ± 0.39	−0.16 ± 0.21
T4	0.135 ± 0.010	19.94 ± 0.21	18.95 ± 0.01	19.98 ± 0.22	−0.17 ± 0.21
T5	0.205 ± 0.010	19.74 ± 0.19	18.60 ± 0.03	19.51 ± 0.21	−0.17 ± 0.21

**Remark*: although in this case the fans were switched off, an air speed of 0.009 m/s was assumed to calculate a Reynolds number greater than zero.

Table 5
Results of dimensionless parameters approach.

Test	*Gr*	*Re*	*Ar*	*Ra*	*Nu (natural)* ($10^4 < Ra < 10^9$)	*Nu (natural)* ($\forall Ra$)	*Nu (forced)* ($Re < 5 \cdot 10^5$)
T1	9.27×10^8	1.07×10^3	812.01	6.78×10^8	95.20	109.43	–
T2	9.96×10^8	7.62×10^3	17.18	7.28×10^8	96.92	111.87	–
T3	8.81×10^8	1.05×10^4	7.95	6.44×10^8	93.98	107.71	61.35
T4	8.42×10^8	1.60×10^4	3.28	6.16×10^8	92.93	106.24	75.70
T5	1.07×10^9	2.43×10^4	1.81	7.82×10^8	98.66	114.35	93.26

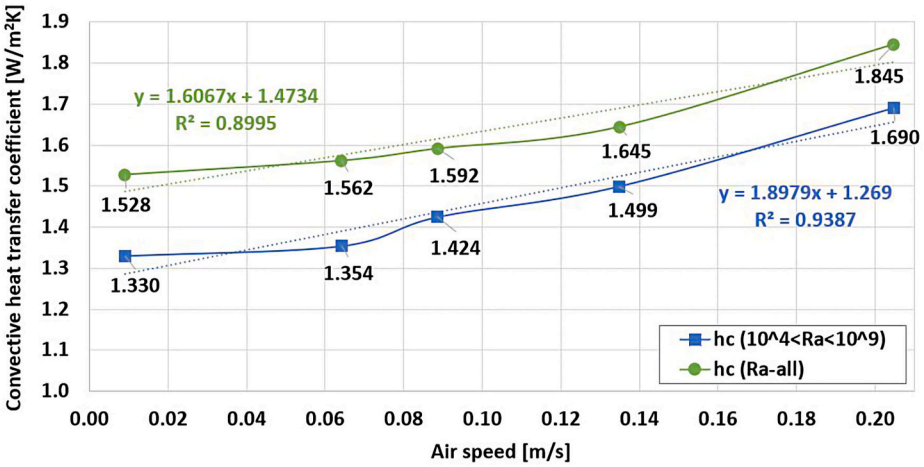

Fig. 4. Convective coefficient (h_c) for different air velocities.

Table 6
Results of radiation coefficients.

Test	T_m [°C]	h_r [W/m^{2}K]
T1	19.61 ± 0.05	5.691 ± 0.003
T2	19.20 ± 0.08	5.667 ± 0.005
T3	19.44 ± 0.20	5.681 ± 0.012
T4	19.47 ± 0.12	5.683 ± 0.007
T5	19.06 ± 0.11	5.659 ± 0.006

Table 7
Results of surface thermal resistance.

Test	h_r [W/m^{2}K]	h_c ($10^4 < Ra < 10^9$) [W/m^{2}K]	$R_{s,i}$ [m^{2}K/W][a]	Variation from ISO 6946[2]	h_c ($Ra\ all$) [W/m^{2}K]	$R_{s,i}$ [m^{2}K/W][a]	Variation from ISO 6946[b]
T1	5.691 ± 0.003	1.330 ± 0.030	0.1301 ± 0.0006	0.11%	1.528 ± 0.047	0.1269 ± 0.0009	−2.41%
T2	5.667 ± 0.005	1.354 ± 0.057	0.1302 ± 0.0011	0.15%	1.562 ± 0.095	0.1268 ± 0.0019	−2.50%
T3	5.681 ± 0.012	1.424 ± 0.095	0.1288 ± 0.0010	−0.96%	1.592 ± 0.126	0.1260 ± 0.0013	−3.05%
T4	5.683 ± 0.007	1.499 ± 0.047	0.1275 ± 0.0010	−1.93%	1.645 ± 0.065	0.1252 ± 0.0013	−3.71%
T5	5.659 ± 0.006	1.690 ± 0.043	0.1249 ± 0.0004	−3.94%	1.845 ± 0.060	0.1225 ± 0.0012	−5.77%

[a] Emissivity factor (E) equal to 0.9.
[b] $R_{s,i}$ equal to 0.13 m^{2}K/W for horizontal heat flow.

$$\frac{\partial R}{\partial x_1} \cong \frac{R(x_1 + \Delta x_1) - R(x_1)}{\Delta x_1} \tag{15}$$

$$\frac{\partial R}{\partial x_2} \cong \frac{R(x_2 + \Delta x_2) - R(x_2)}{\Delta x_2} \tag{16}$$

These values can be used in Eq. (10) for computing the uncertainty in the result.

3. Results

Steady-state operating conditions were reached during the experimental campaigns. The average values measured for air velocity, surface and air temperatures are summarized in Table 4.

The dimensionless parameters approach, considering a kinematic viscosity equal to 1.516×10^{-5} m^2/s (for *film* temperature of about 20 °C) and a Prandtl number equal to 0.731 [24], allowed to obtain the results shown in Table 5. Natural convection occurs for cases T1 and T2, while the other tests are characterized by mixed convection.

All the parameters necessary to determine h_c as the air speed varies for the investigated tests are therefore known, as shown in Fig. 4.

Considering the emissivity of sample wall surface and baffle, equal to 0.94 and 0.95, respectively, and the mean radiant absolute temperatures (T_m) (Eq. (8)), the radiative coefficients are determined, as shown in Table 6.

Based on the determined convective and radiative coefficients, R_s (Eq. (2)) with different air velocities can be found. The achieved results are summarized in Table 7 and Fig. 5. Two equations able to correlate h_c and air velocity can be identified, with R^2 values of about 0.90 (for the equation based on a Ra between 10^4 and 10^9) and 0.94 (for the equation relevant $\forall Ra$). Applying the equation based on a Ra number between 10^4 and 10^9, the h_c ranges from 1.528 W/m^{2}K to 1.845 W/m^{2}K. Comparing these values with the constant convective coefficient suggested by the ISO 6946, it is possible to observe percentage differences ranging from −38.9% to −26.2%. On the other hand, by using the equation relevant $\forall Ra$, the h_c ranges from 1.330 W/m^{2}K to 1.690 W/m^{2}K, with variations from −46.8% to −32.4%. These outcomes were then applied in terms of $R_{s,i}$, finding percentage differences ranging from −3.94% to +0.15% with the

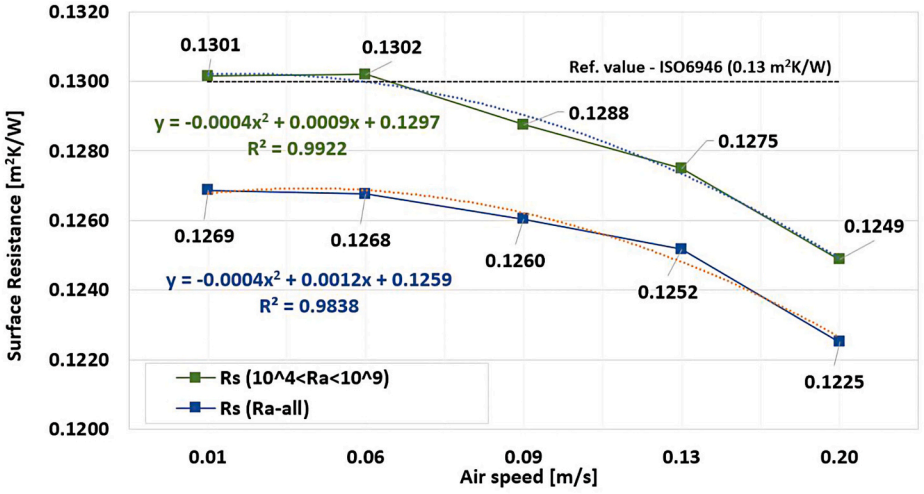

Fig. 5. Surface thermal resistance ($R_{s,i}$) for different air velocities.

Table 8
Results on convective coefficients comparison.

Reference	h_c [W/m^{2}K]	$R_{s,i}$ [m^{2}K/W]	Variation from ISO 6946[a]
Test T1 (10^4<Ra<10^9)	1.330	0.1301	0.11%
Test T1 (Ra all)	1.528	0.1269	−2.41%
ASHRAE (10^5<Ra<10^9)	1.173	0.1328	2.19%
ASHRAE (Ra<10^9)	1.297	0.1307	0.54%
Churchill and Chu (1)	1.165	0.1330	2.30%
Churchill and Chu (2)	0.296	0.1504	15.68%
Khalifa and Marshall (1)	2.348	0.1149	−11.61%
Khalifa and Marshall (2)	2.984	0.1071	−17.62%

[a] $R_{s,i}$ equal to 0.13 m^{2}K/W.

equation based on a *Ra* between 10^4 and 10^9. On the other hand, by applying the equation relevant $\forall Ra$, percentage variations ranging from −5.77% to −2.41% were highlighted.

The results obtained from comparison with the existing correlations for the convective coefficient are shown in Table 8.

4. Conclusions

The effects of environmental boundary conditions on the wall surface heat transfers were investigated in a GHB. All the needed parameters for the convective and radiative coefficients identification were acquired under steady-state boundary conditions, considering different air flows. Under natural convection conditions, *Nu* can be computed in function of the *Ra* number, but different formulas can be applied. However, finding the proper h_c value is challenging, needing an appropriate experimental equipment. Currently, many established correlations can be found in literature. Here, six established correlations were applied, expressed as a function of temperature difference (air-surface) and wall height.

By comparing the experimental results and the values suggested by the ISO 6946, it can be observed that lower experimental convective coefficients were obtained. The comparison among the experimental h_c and the constant value suggested by the standard provides percentage differences ranging between −46.8% and −32.4%. It is worthy to observe that lower convective coefficients values are here balanced by higher radiative coefficients values, thus leading to reduced percentage differences in terms of surface thermal resistance. Moreover, due to the thermal and fluid dynamic phenomena, the hot wire anemometer position needs to be better investigated for better comprehending the influence on h_c coefficients. Nevertheless, convective and radiative heat transfers in real environments could lead to higher deviations. Consequently, this issue needs to be further investigated, to provide much more findings for indirect heat flow measurements techniques. It is worth pointing out that the number of sensors used, and their installation height allowed to calculate local heat transfer coefficients. A greater number of probes, installed at different heights, can lead to a wider assessment of the heat transfer coefficients along the wall surface, according to the thermal and fluid dynamic phenomena induced by the fans. The proposed method based on dimensionless parameters could be applied for those quite new experimental techniques, such as the thermometric method [10] which requires the total air-wall heat transfer coefficient knowledge.

Funding

This research did not receive any specific grant from funding agencies in the public, commercial, or not-for-profit sectors.

Authors statement

Tullio de Rubeis: Conceptualization, Methodology, Formal Analysis, Investigation, Writing – Original Draft.
Luca Evangelisti: Conceptualization, Methodology, Formal Analysis, Writing – Original Draft.
Claudia Guattari: Methodology, Formal Analysis, Writing – Original Draft.
Pierluigi De Berardinis: Investigation, Writing - Review & Editing, Supervision.
Francesco Asdrubali: Investigation, Resources, Writing - Review & Editing, Supervision.
Dario Ambrosini: Investigation, Resources, Writing - Review & Editing, Supervision.

Declaration of competing interest

The authors declare that they have no known competing financial interests or personal relationships that could have appeared to influence the work reported in this paper.

References

[1] H. Hou, X. Feng, Y. Zhang, H. Bai, Y. Ji, H. Xu, Energy-related carbon emissions mitigation potential for the construction sector in China, Environ. Impact. Asses. 89 (2021), 106599.
[2] International Energy Agency (IEA), World Energy Outlook, IEA, Paris, France, 2016, 2016.
[3] International Energy Agency (IEA), CO2 Emissions from Fuel Combustion. Beyond 2020 Online Database, International Energy Agency, Paris, 2012, p. 135, 2012.
[4] European Commission, The European Green Deal, COM, 2019, p. 640, final, Brussel 11.12.2019.
[5] P.G. Cesaratto, M. De Carli, A measuring campaign of thermal conductance in situ and possible impacts on net energy demand in buildings, Energy Build. 59 (2013) 29–36.
[6] E. Sassine, A practical method for in-situ thermal characterization of walls, Case Stud. Therm. Eng. 8 (2016) 84–93.
[7] C. Cornaro, V. Adoo Puggioni, R.M. Strollo, Dynamic simulation and on-site measurements for energy retrofit of complex historic buildings: villa Mondragone case study, J. Build. Eng. 6 (2016) 17–28.
[8] A. Alazazmeh, M. Asif, Commercial building retrofitting: assessment of improvements in energy performance and indoor air quality, Case Stud. Therm. Eng. 26 (2021), 100946.
[9] M. Teni, H. Krstic, P. Kosinski, Review and comparison of current experimental approaches for in-situ measurements of building walls thermal transmittance, Energy Build. 203 (2019), 109417.
[10] D. Bienvenido-Huertas, J. Moyano, D. Marin, R. Fresco-Contreras, Review of in situ methods for assessing the thermal transmittance of walls, Renew. Sustain. Energy Rev. 102 (2019) 356–371.
[11] S.-H. Kim, J.-H. Kim, H.-G. Jeong, K.-D. Song, Reliability field test of the air-surface temperature ratio method for in situ measurement of U-values, Energies 11 (2018) 1–15.
[12] L. Evangelisti, C. Guattari, T. de Rubeis, Preliminary analysis of the influence of environmental boundary conditions on convective heat transfer coefficients, J. Phys. Conf. Ser. 1868 (2021), 012024.
[13] L. Peeters, I. Beausoleil-Morrison, A. Novoselac, Internal convective heat transfer modeling: critical review and discussion of experimentally derived correlations, Energy Build. 43 (2011) 2227–2239.

[14] W. Yang, X. Zhu, J. Liu, Annual experimental research on convective heat transfer coefficient of exterior surface of building external wall, Energy Build. 155 (2017) 207–214.
[15] S. Obyn, G. van Moeseke, Variability and impact of internal surfaces convective heat transfer coefficients in the thermal evaluation of office buildings, Appl. Therm. Eng. 87 (2015) 258–272.
[16] A.-J.N. Khalifa, Natural convective heat transfer coefficient e a review: I. Isolated vertical and horizontal surfaces, Energy Convers. Manag. 42 (2001) 491–504.
[17] M. Mirsadeghi, D. Costola, B. Blocken, J.L.M. Hensen, Review of external convective heat transfer coefficient models in building energy simulation programs: implementation and uncertainty, Appl. Therm. Eng. 56 (2013) 134–151.
[18] L. Evangelisti, C. Guattari, P. Gori, R. de Lieto Vollaro, F. Asdrubali, Experimental investigation of the influence of convective and radiative heat transfers on thermal transmittance measurements, Int. Commun. Heat Mass Tran. 78 (2016) 214–223.
[19] D. Bienvenido-Huertas, J. Bermúdez, J.J. Moyano, D. Marín, Influence of ICHTC correlations on the thermal characterization of façades using the quantitative internal infrared thermography method, Build. Environ. 149 (2019) 512–525.
[20] M. Camci, Y. Karakoyun, O. Acikgoz, A.S. Dalkilic, A comparative study on convective heat transfer in indoor applications, Energy Build. 242 (2021), 110985.
[21] P. Michalak, Experimental and theoretical study on the internal convective and radiative heat transfer coefficients for a vertical wall in a residential building, Energies 14 (2021) 5953.
[22] ISO 6946 - Building Components and Building Elements - Thermal Resistance and Thermal Transmittance - Calculation Methods, 2017.
[23] UNI EN ISO 8990, Thermal Insulation - Determination of Steady-State Thermal Transmission Properties - Calibrated and Guarded Hot Box, 1999.
[24] T.L. Bergman, A.S. Lavine, F.P. Incropera, D.P. Dewitt, Fundamentals of Heat and Mass Transfer, John Wiley & Sons, 2017, 13 978-0470-50197-9.
[25] S. Churchill, H. Chu, Correlating equations for laminar and turbulent free convection from a vertical plate, Int. J. Heat Mass Tran. 18 (1975) 1323–1329.
[26] F. Alamdari, G. Hammond, Improved data correlations for buoyancy-driven convection in rooms, Build. Serv. Eng. Technol. 4 (1983) 106–111.
[27] A. Khalifa, R. Marshall, Validation of heat transfer coefficients on interior building surfaces using real-sized indoor test cell, Int. J. Heat Mass Tran. 33 (1990) 2219–2236.
[28] H. Awbi, A. Hatton, Natural convection from heated room surfaces, Energy Build. 30 (1999) 233–244.
[29] N. Walikewitz, M. Langner, F. Meier, W. Endlicher, The difference between the mean radiant temperature and the air temperature within indoor environments: a case study during summer conditions, Build. Environ. 84 (2015) 151–161.
[30] E. Barreira, R.M.S.F. Almeida, M.L. Simões, Emissivity of building materials for infrared measurements, Sensors 21 (2021) 1961.
[3][1]] T. de Rubeis, I. Nardi, M. Muttillo, Development of a low-cost temperature data monitoring. An upgrade for hot box apparatus, J. Phys. Conf. Ser. 923 (2017), 012039.
[32] T. de Rubeis, M. Muttillo, I. Nardi, L. Pantoli, V. Stornelli, D. Ambrosini, Integrated measuring and control system for thermal analysis of buildings components in hot box experiments, Energies 12 (2019) 2053.
[33] J.P. Holman, Experimental Methods for Engineers, eighth ed.; McGraw-Hill series in mechanical engineering; ISBN-13: 978-0-07-352930-1.